Analysis and Control of Harmonic Radiation From Active Integrated Oscillator Antennas

Martin J. Cryan, *Senior Member, IEEE*, G. R. Buesnel, and Peter S. Hall, *Fellow, IEEE*

Abstract—Harmonic radiation from microstrip patch oscillators is examined experimentally and theoretically using both a single and dual parallel-tuned circuit Van der Pol oscillator model. Closed-form expressions are obtained for the fundamental and first harmonic voltage amplitudes, and results show reasonably good agreement with a commercial circuit simulator. Such expressions will be useful for designers of active integrated antennas, giving them greater physical insight into their operation. Experimental results are presented for three configurations of a patch oscillator, i.e., rectangular patch, circular-sector patch, and quarter-wave shorted patch. The latter two configurations present very low resistance at the first harmonic frequency and this leads to improved harmonic suppression performance. This is in qualitative agreement with theoretical predictions.

Index Terms—Active integrated antennas, antennas, harmonic radiation.

I. INTRODUCTION

FUTURE systems employing active antennas will require very low levels of harmonic radiation in order to meet electromagnetic compatibility specifications. Active antennas introduce nonlinear devices directly into the antenna and, thus, they can exhibit high levels of harmonic radiation. Moreover, due to size constraints, filters cannot be easily added, as in conventional systems. In the case of active receiving antennas, it seems that, by suppressing the harmonic resonances of the antenna, the harmonic reception problem can be reduced [1], [2]. However, with patch oscillators, due to the interdependence of the active device and patch, the solution to the problem of harmonic radiation is more complex and it may be approached in two ways. Firstly, out-of-band radiation from the active integrated oscillator can be minimized at the design stage by control of the impedance presented by the antenna to the oscillator. Secondly, it may be controlled once the device has been constructed by the use of frequency-selective surfaces [3]. This paper concentrates on the first approach. Firstly, a theoretical analysis is presented, which gives the designer insight into the amount of harmonic suppression obtainable for a given first harmonic antenna input resistance. This paper then presents experimental results, which show the levels of suppression that are obtainable with three different configurations of a patch oscillator. Firstly, a radiative edge-fed rectangular patch oscillator, where the an-

tenna will have relatively high input resistance, at the first harmonic frequency. Secondly, two examples of patch oscillators using antennas with low first harmonic input resistance, i.e., a circular-sector patch and a quarter-wave shorted patch.

II. ANALYSIS AND SIMULATION

Several methods have been suggested for analysis and simulation of active integrated antennas [4]. Very simple equivalent-circuit models have been used to allow dynamic modeling of arrays [5], while more accurate active device equivalent circuits have been linked to the method of moments [6] and finite-difference time-domain (FDTD) method [7]. The very simple models allow analytical expressions to be derived that give great insight into performance mechanisms. The more accurate full-wave models are computationally intensive. In this paper, the extension of simple models to the prediction of harmonic radiation is explored with the aim of extracting analytic expressions and design insight.

Firstly, a single parallel-tuned circuit is used to model the fundamental resonance of a microstrip patch oscillator to allow simple expressions for harmonic levels to be obtained. This is described in Section III. However, this simple model is found not to adequately model the harmonic behavior of the patch oscillator. The model can be improved by including higher order resonances of the patch antenna. Since these often occur at harmonic intervals, they will be likely to have large effects on harmonic radiation. This is achieved by adding a second parallel-tuned circuit in series with the first. This is described in Section IV.

Some comments on the analytical solution can be made. The solution proceeds by obtaining a differential equation, which describes the behavior of the circuit. In the case of the single parallel-tuned circuit model, this is nonlinear and of second order. For the dual circuit, a fourth-order equation is obtained. There are a number of methods that can be employed to solve this problem analytically. It should be noted that, not only is a solution at the fundamental frequency required, but a solution at the first harmonic is also needed. This requirement limits the approaches that can be taken.

Initially, a perturbation method was considered [8]. This allows the investigation of weakly nonlinear systems and was used by Van der Pol [9] to investigate the steady-state solution for triode generators. It assumes that the solution can be written in terms of a polynomial in powers of a small parameter that describes the strength of the nonlinearity. By back substitution, the original equation can be rewritten as a series of simultaneous linear equations, which may be solved recursively. For the case of a second-order nonlinear equation, this approach gives
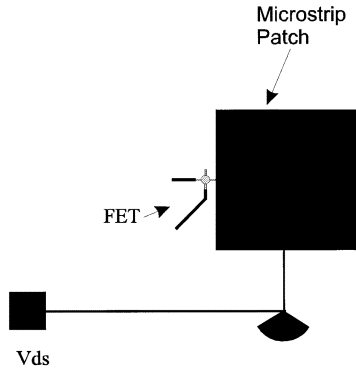
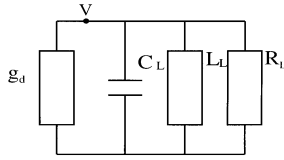Fig. 1.   Basic configuration of a microstrip patch oscillator.

Fig. 2.   Single LCR model for a microstrip patch oscillator.

reasonable results. However, as the model becomes more detailed, this approach becomes rather cumbersome. An elegant approach, also shown by Van der Pol [9], [10], involves assuming a form for the steady-state solution and substituting this back into the original equation. This may then be rewritten as a sum of sine and cosine terms, the coefficients of which can be formed into a set of simultaneous equations. This method is elegant since it automatically gives solutions for the fundamental and first harmonic and, in principle, for any number of harmonics. The Mathematica software package has been used to expand the differential equations in terms of sines and cosines and to obtain solutions for the nonlinear simultaneous equations.

III. SINGLE RESONATOR CASE

A. Analysis

An example of an active antenna is shown in Fig. 1. The drain of a field-effect transistor is connected to the edge of a microstrip patch, which acts as both the resonant load for the oscillator and a radiating element. The source and gate are loaded with short-circuit transmission lines in order to obtain a negative resistance at the drain port. The oscillator was designed using Hewlett-Packard's Microwave Design System (MDS). Both the linear and nonlinear oscillator design tools were used in combination with a transmission-line model of the patch antenna [11]. The design procedure and a typical schematic layout is presented in [12].

A Van der Pol analysis of the patch oscillator was performed using a simple parallel-tuned circuit to model the patch and a nonlinear negative resistance to model the field-effect transistor, as shown in Fig. 2. The values of L, C, and R are found by fitting the model to the measured input impedance of the antenna. The voltage differential equation for a single LCR circuit is

$$\frac{d^2 V}{dt^2} + \frac{dV}{dt}\frac{(g_d + G_L)}{C_L} + V\omega_0^2 = 0 \tag{1}$$

where g_d is the nonlinear conductance derived from the current–voltage relationship shown in (2). A cubic polynomial is the minimum order required to obtain stable oscillation conditions [13]

$$I = -g_0 V + g_1 V^2 + g_2 V^3. \tag{2}$$

Differentiating (2) with respect to V, we obtain

$$g_d = -g_0 + 2g_1 V + 3g_2 V^2. \tag{3}$$

Also, $\omega_0^2 = 1/\sqrt{L_L C_L}$ and $G_L = 1/R_L$.

It is reasonable to assume the solution of (1) to be a sum of sinusoids, and assuming that terms above the first harmonic can be neglected (comparison with numerical simulation in Section III-B will show this to be valid), we obtain

$$V = a_1 \sin(\omega_0 t) + a_2 \sin(2\omega_0 t). \tag{4}$$

This is now substituted in (1), and since steady-state solutions are required, it is assumed that

$$\frac{da_i}{dt} = \frac{d^j a_i}{dt^j} = 0, \qquad i = 1, 2; \quad j = 1, \ldots, n.$$

The result is expanded and an equation with the following form is obtained:

$$A\cos(\omega_0 t) + B\sin(\omega_0 t) + C\cos(2\omega_0 t) + D\sin(2\omega_0 t) = 0. \tag{5}$$

Since these four terms are orthogonal, the coefficients A, B, C, and D of (5) can be equated to zero, resulting in four simultaneous equations for a_1 and a_2. Only two of these equations are required and, in this case, the correct solutions have been obtained using the equations from coefficients A and D. If $a_2 \ll a_1$, which is true for most oscillators, the following expressions are obtained:

$$a_1 = \sqrt{\frac{4(g_0 - G_L)}{3g_2}} \tag{6}$$

and

$$a_2 = \frac{a_1^2 g_1}{3\omega_0 C_L}. \tag{7}$$

From (6), it is seen that a_1 is real only when $g_0 > G_L$. This is, in fact, the well-known small-signal oscillation startup criteria for parallel resonant circuits and, equivalently, $r_0 > R_L$ for series resonant circuits [14]. Equation (7) shows that the level of the first harmonic is proportional to g_1, which seems intuitively correct since (2) shows that first harmonic terms are generated by the V^2 term involving g_1. Remembering that the quality factor of a parallel LCR circuit is given by

$$Q = \omega CR \tag{8}$$

it may be observed that the level of the first harmonic (a_2) is inversely proportional to the Q of the resonator. This highlights an immediate problem when using microstrip patches as resonators since, the higher the Q of the patch, the poorer its antenna performance in terms of bandwidth and, hence, frequency
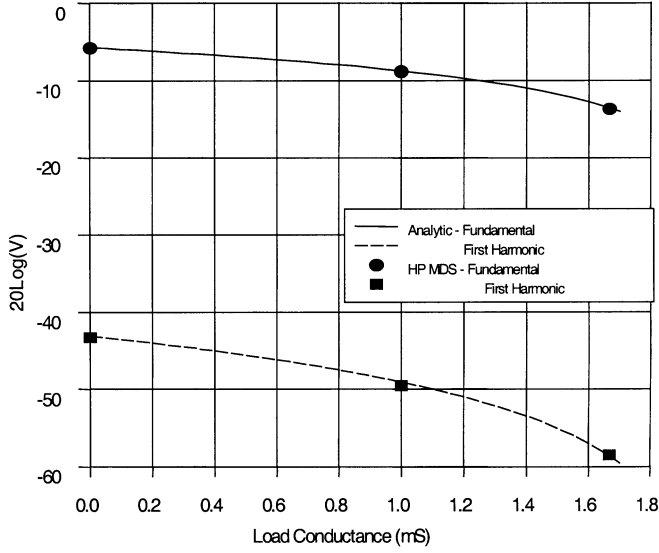
Fig. 3. Voltage amplitudes for fundamental (a_1) and first harmonic (a_2) oscillations versus load conductance (G_L) for a single LCR circuit. ($g_0 = 2$ mS, $g_1 = 5$ mS, $g_2 = 10$ mS, $C_L = 4$ pF, $L_L = 1$ nH. Analysis: — fundamental, - - - first harmonic. Simulation (HP MDS), ● fundamental, ■ first harmonic).

tuning. Thus, a compromise between antenna performance and harmonic level may well be required.

B. Numerical Results

In order to validate these results, a Van der Pol oscillator has been implemented using the Hewlett-Packard MDS harmonic-balance simulator. To obtain typical values for the conductance coefficients of (3), a harmonic-balance analysis with swept input power was performed in order to determine the input admittance at the drain of the oscillator with the patch removed. Coefficients were extracted by fitting a polynomial to the real part of the admittance-voltage data at a single frequency. A symbolically defined device (SDD) was then used within MDS to simulate the nonlinear conductance. Results for harmonic levels with respect to G_L are shown in Fig. 3. Good agreement has been obtained between the closed-form expressions and MDS. This validates the analysis method and shows that the assumptions made were reasonable. It is seen that, as the load conductance approaches the value of the device negative conductance, the level of the first harmonic decreases, and this is consistent with the concept of a low-perturbation oscillator design approach. The levels of the first harmonic shown are very low and, indeed, much lower than values typically obtained for patch oscillators (see Section V). This suggests that a single parallel-tuned circuit does not adequately model the patch. The model can be improved by taking into account the first higher order resonance of the patch antenna.

IV. DUAL-RESONATOR CASE

In order to model the first higher order resonance of a microstrip patch, a second parallel-tuned circuit is added in series, as shown in Fig. 4. The voltage differential equation for the dual
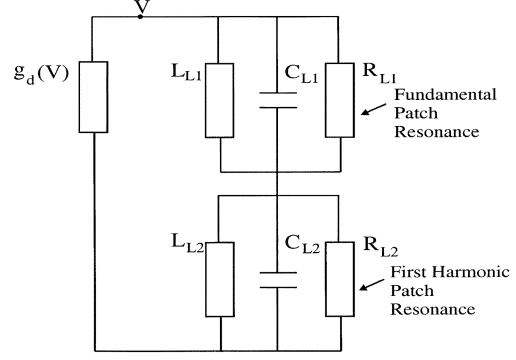

Fig. 4. Dual LCR model for a microstrip patch oscillator.

LCR circuit is now fourth order as follows:

$$\frac{d^4V}{dt^4} + \frac{d^3V}{dt^3}\left(\frac{g_d}{C_{L1}} + \frac{g_d}{C_{L2}} + \alpha_1 + \alpha_2\right)$$
$$+ \frac{d^2V}{dt^2}\left(g_d\left(\frac{\alpha_2}{C_{L1}} + \frac{\alpha_1}{C_{L2}}\right) + \alpha_1\alpha_2 + \omega_1^2 + \omega_2^2\right)$$
$$+ \frac{dV}{dt}\left(g_d\left(\frac{\omega_2^2}{C_{L1}} + \frac{\omega_1^2}{C_{L2}}\right) + \alpha_2\omega_1^2 + \alpha_1\omega_2^2\right)$$
$$+ V\omega_1^2\omega_2^2 = 0 \qquad (9)$$

where $\alpha_i = 1/R_{Li}C_{Li}$ and $\omega_i = \sqrt{1/L_{Li}C_{Li}}$, $i = 1, 2$ and where g_d is given by (3).

Equation (9) shows the large increase in complexity incurred by introducing a second resonance in the model. It is no longer possible to obtain solutions using the procedure for the single-resonator case. In order to proceed, a solution for the fundamental amplitude is first sought. It is assumed that $a_2 \ll a_1$ and, thus, the solution may be approximated by a single cosinusoidal term

$$V = a_1 \cos(\omega_0 t). \qquad (10)$$

Equation (10) is now substituted in (9). The result is expanded as before and, since there is only one unknown, only one equation is required, for which correct solutions are obtained using coefficient B. The solution for a_1 is

$$a_1 = \sqrt{\frac{4\left(g_0 - \frac{1}{R_{L1}}\right)}{3g_2}}. \qquad (11)$$

This is seen to be of the same form as for the single-resonator case and depends only on the fundamental resonant circuit resistance R_{L1}. This approximation can now be used to obtain a solution for the harmonic voltage amplitude a_2.

In the single-resonator case, the full solution is written as the sum of the fundamental and first harmonic sinusoids. However, using this in the dual-resonator case produces insoluble simultaneous equations. It was found to be necessary to include a second harmonic term in order to proceed. Thus, the form of the solution is

$$V = a_1 \cos(\omega_0 t) + a_2 \cos(2\omega_0 t) + a_3 \cos(3\omega_0 t). \qquad (12)$$

If (12) is now substituted in (9) and expanded in sines and cosines, four simultaneous equations are obtained. Assuming $a_2 \ll a_1$ and $a_3 \ll a_1$, we can ignore terms in $a_2 a_3$, a_2^3, and a_3^2, giving

$$
\begin{aligned}
A = {} & 4 + 9a_1^2 g_2 R_{L1} + 33a_1 a_3 g_2 R_{L1} + 9a_1^2 g_2 R_{L2} \\
& + 33a_1 a_3 g_2 R_{L2} - 4g_o (R_{L1} + R_{L2}) \\
& + 20a_2 g_1 (R_{L1} + R_{L2}) + 54a_2^2 g_2 (R_{L1} + R_{L2})
\end{aligned} \tag{13a}
$$

$$
\begin{aligned}
B = {} & 4g_0 C_{L2} + 4a_2 g_1 C_{L2} + 8a_2 g_1 C_{L1} - 3a_1^2 g_2 C_{L2} \\
& - 6a_2^2 g_2 C_{L2} + 21a_1 a_3 g_2 C_{L2} + 24a_1 a_3 g_2 C_{L1} - \frac{4a_1 C_{L2}}{R_{L1}}
\end{aligned} \tag{13b}
$$

$$
\begin{aligned}
C = {} & 4a_2 g_0 R_{L2} - a_1^2 g_1 R_{L2} - 10a_1 a_3 g_1 R_{L2} - 9a_1^2 a_2 g_2 R_{L2} \\
& + 4a_2 g_0 R_{L1} - a_1^2 g_1 R_{L1} - 10a_1 a_3 g_1 R_{L1} - 9a_1^2 a_2 g_2 R_{L1} \\
& - 4a_2
\end{aligned} \tag{13c}
$$

$$
\begin{aligned}
D = {} & -2a_2 g_0 C_{L1} - a_1^2 g_1 C_{L2} + 6a_1 a_3 g_1 C_{L2} + 8a_1 a_3 g_1 C_{L1} \\
& + 3a_1^2 a_2 g_2 C_{L1} + \frac{2a_2 C_{L1}}{R_{L2}}.
\end{aligned} \tag{13d}
$$

Proceeding as for the single-resonator case, the assumption of steady state allows (13) to be equated to zero. Solving for a_2 and a_3 and substituting in the approximate solution for a_1 in (11), a solution for the first harmonic is found in (14), shown at the bottom of this page, where $R_t = R_{L1} + R_{L2}$ and $R_f = -1 + g_0 R_t$

The closed-form expressions for a_1 and a_2 were again compared with MDS. The results are shown in Fig. 5. The fundamental oscillator output voltage is plotted against input resistance at the fundamental frequency. The range of resistance is typical for microstrip patches. The first harmonic amplitude is also plotted at two different first harmonic input resistances. The conductance coefficients have been recalculated at a different bias point in order to allow more realistic patch input impedances to be used, i.e., between 500–50 Ω. The agreement between the analytic expressions and MDS for the fundamental is very good and the agreement for the first harmonic is reasonable across a wide range of input resistance values. These results seem intuitively correct since, as the first harmonic resistance approaches zero, the first harmonic amplitude reduces. Some typical measured results are also shown as the circle—funda-
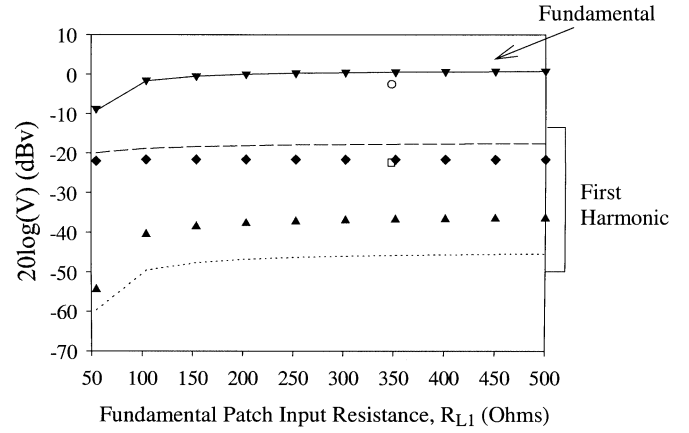

Fig. 5. Voltage amplitudes for fundamental (a_1) and first harmonic (a_2) oscillations versus fundamental load resistance (R_{L1}) in dual LCR circuit for analytic expressions, MDS harmonic balance and typical measured values $g_0 = 20$ mS, $g_1 = 5$ mS, $g_2 = 20$ mS, $C_1 = 20$ pF, $L_1 = 0.2$ nH, $C_2 = 20$ pH, $L_2 = 0.05$ nH, $R_{Li} = 1/G_{Li}$. Analysis: —— fundamental, - - - first harmonic $R_{L2} = 50$, first harmonic $R_{L2} = 5$. Simulation (HP-MDS): ▼ fundamental, ◆ first harmonic $R_{L2} = 50$, ▲ first harmonic $R_{L2} = 5$. Measurement: ○ fundamental, □ first harmonic.

mental and square—first harmonic. These show that the theoretical results are similar to those found with practical oscillators. The results show that lowering the resistance will reduce the amplitude of the first harmonic. This agrees with the results found for receive-type active antennas [1], [2]. Thus, the analytical expressions give reasonable agreement with measurement, agree with intuitive understanding of oscillator action, and provide a useful first-order design tool. A further development would be to include the nonlinear susceptance of the oscillator circuit. It might still be possible to obtain closed-form expressions, and this would result in a much more accurate model for the patch oscillator.

V. EXPERIMENTAL RESULTS

A series of experiments were carried out to determine the degree of harmonic suppression that could be achieved using microstrip patch oscillators. Three types of patch geometry were used. Fig. 6 shows a rectangular radiating edge fed arrangement. Fig. 7 shows a circular-sector patch of design proposed by Radisic et al. [2]. Fig. 8 shows a quarter-wave shorted rectangular design. The antennas were all fabricated on a substrate of relative permittivity 2.2 and height $= 0.508$ mm and the MESFET device chosen was the Hewlett-Packard HP ATF 26884. The

$$
\begin{aligned}
a_2 = {} & \frac{60 C_{L2} g_1^2 R_{L2} R_t + C_{L1} \left(80 g_1^2 R_{L2} R_t + 11 g_2 \left(-3R_{L1} + R_{L2} R_f \right) \right)}{108 (4C_{L1} + 3C_{L2}) g_1 g_2 R_{L2} R_t} \\
& + \frac{\sqrt{-144 C_{L2}^2 g_1^2 R_{L2}^2 R_t \left(-25 g_1^2 R_t + 33 g_2 R_f \right)}}{108 (4C_{L1} + 3C_{L2}) g_1 g_2 R_{L2} R_t} + \frac{\sqrt{C_{L1}^2 \left(80 g_1^2 R_{L2} R_t + 11 g_2 \left(-3R_1 + R_{L2} R_f \right) \right)^2}}{108 (4C_{L1} + 3C_{L2}) g_1 g_2 R_{L2} R_t} \\
& \cdot \frac{\sqrt{-24 C_{L1} C_{L2} g_1^2 R_{L2} R_t \left(-400 g_1^2 R_{L2} R_t + 11 g_2 \left(15 R_{L1} + 19 R_{L2} R_f \right) \right)}}{108 (4C_{L1} + 3C_{L2}) g_1 g_2 R_{L2} R_t}
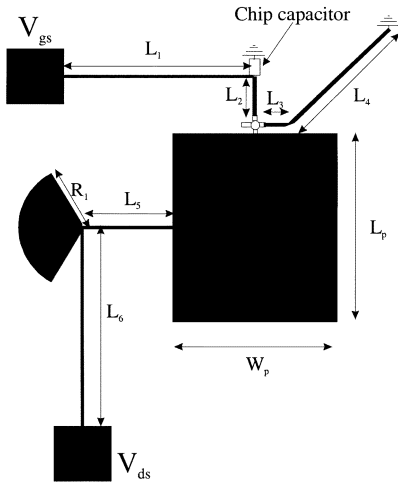\end{aligned} \tag{14}
$$

Fig. 6. End-fed rectangular patch oscillator with MESFET (Agilent ATF26884) $W_p = 20.0$ mm, $L_p = 24.0$ mm, $L_1 = 24.5$ mm, $L_2 = 5.0$ mm, $L_3 = 2.5$ mm, $L_4 = 16.5$ mm, $L_5 = 11.5$ mm, $L_6 = 25$ mm. Widths: L_1, L_5, $L_6 = 0.2$ mm, L_2, L_3, $L_4 = 0.5$ mm. $R_1 = 8$ mm, radial stub angle $= 120°$. Square bias pads, 7.0 mm $\times$ 7.0 mm.
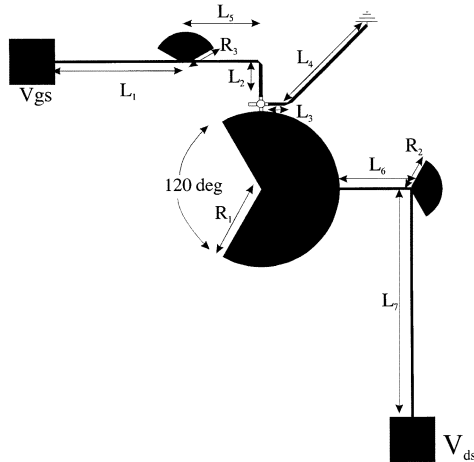

Fig. 7. Circular-sector patch oscillator with MESFET (Agilent ATF26884) $R_1 = 12.0$ mm, $L_1 = 20.0$ mm, $L_2 = 5.0$ mm, $L_3 = 2.5$ mm, $L_4 = 16.5$ mm, $L_5 = 11.0$ mm, $L_6 = 11.0$ mm, $L_7 = 35.0$ mm. Widths: L_6, $L_7 = 0.2$ mm, L_1, L_2, L_3, L_4, $L_5 = 0.5$ mm, $R_2 = 5.0$ mm, radial stub angle $= 120°$, $R_3 = 5.0$ mm, radial stub angle $= 120°$. Square bias pads, 7.0 mm $\times$ 7.0 mm.
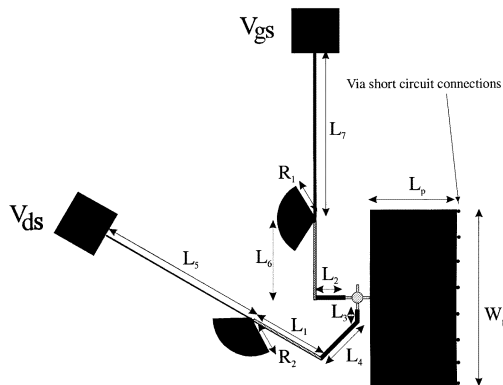

Fig. 8. Rectangular quarter-wave shorted patch oscillator with MESFET (Agilent ATF26884) $W_p = 20.0$ mm, $L_p = 12.0$ mm, $L_1 = 11.0$ mm, $L_2 = 5.0$ mm, $L_3 = 2.5$ mm, $L_4 = 16.5$ mm, $L_5 = 20.0$ mm, $L_6 = 11.0$ mm, $L_7 = 20.0$ mm. Widths: L_1, L_5, L_6, $L_7 = 0.2$ mm, L_2, L_3, $L_4 = 0.5$ mm, $R_1 = 5.0$ mm, radial stub angle $= 120°$, $R_2 = 5.0$ mm, radial stub angle $= 120°$. Square bias pads, 7.0 mm $\times$ 7.0 mm.
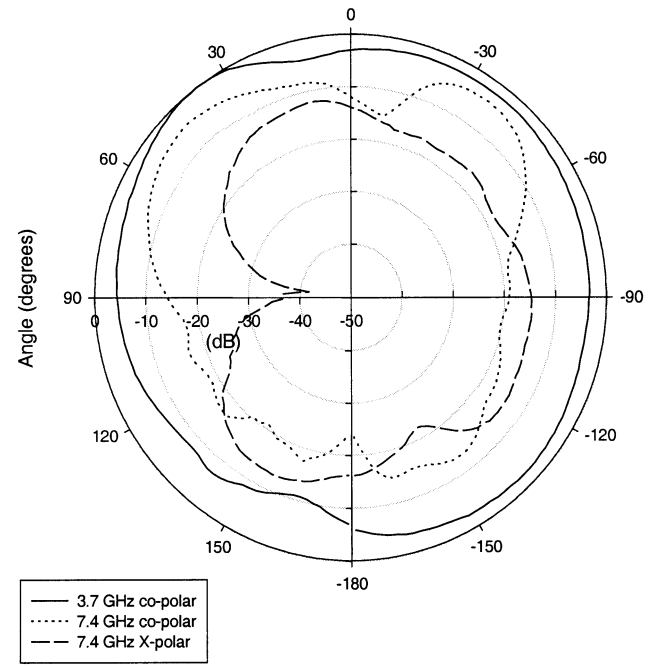

Fig. 9. E-plane radiation patterns generated by end-fed rectangular patch oscillator of Fig. 6 $V_{ds} = 2.5$ V.

patch antennas were all designed to be resonant near to 4 GHz. The same oscillator circuit was used as shown in [12] with the addition of a gate-bias line to increase the tunability of the circuits. Drain bias was provided using radial stub bias networks. Gate bias was provided with radial stub bias networks for the circular-sector and quarter-wave shorted patch and with a surface-mount chip capacitor for the rectangular patch. In all cases, the ground planes were approximately 70 mm $\times$ 70 mm.

The patch oscillators under test were mounted in an anechoic chamber and placed 1.0 m away from a wide-band receiving antenna, which was connected to an HP83006 0–26.5-GHz amplifier. The output of the amplifier was connected to the HP8560E spectrum analyzer. A personal computer was used to automatically control the experiments and record the output data. In all cases, the oscillator bias conditions were adjusted to obtain the best harmonic suppression. The radiation patterns for these patch oscillators were measured in 2° steps through a full 360° arc, in both co- and cross-polarizations at both fundamental and first harmonic frequencies. Since the cross-polar result at the fundamental frequency was always lower than the co-polar result, the data is omitted for clarity.

A. Fundamental and Harmonic Radiation Patterns

Figs. 9 and 10 show the E- and H-plane radiation for the end-fed rectangular patch of Fig. 6. The fundamental E-plane pattern agrees reasonably well with that expected for a rectangular patch. There is however a beam squint to 40° and the front-to-back ratio is quite poor. These could be caused by radiation from the gate and drain transmission lines and from the chip capacitor ground connection at the gate line. The harmonic levels can be seen to be very high, in some case, only 1 dB lower than the fundamental at boresight. The H-plane patterns are shown in Fig. 10. The fundamental pattern is quite poor and
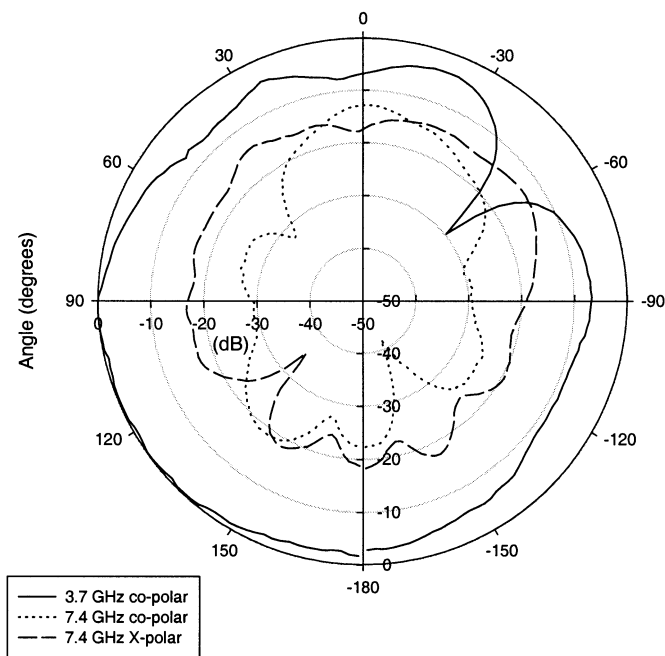
Fig. 10. H-plane radiation patterns generated by end-fed rectangular patch oscillator of Fig. 6 $V_{\mathrm{ds}} = 2.5$ V.
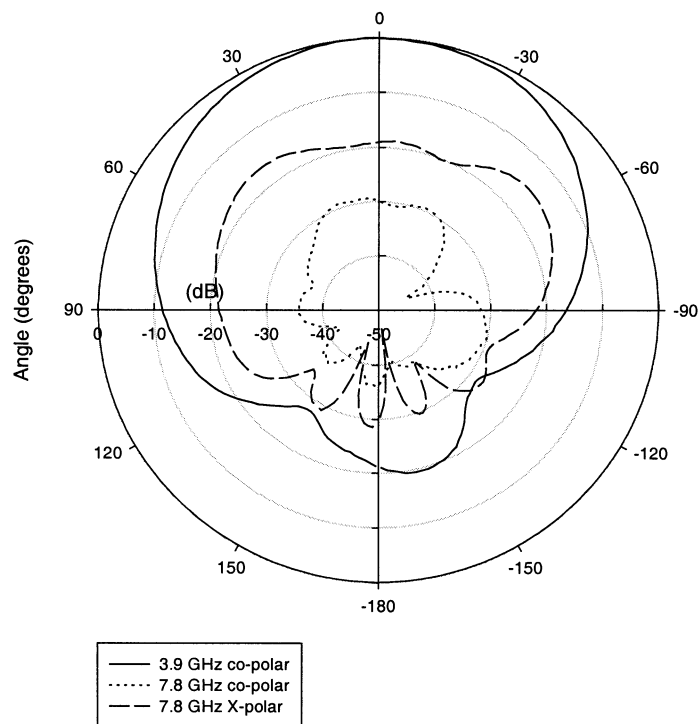

Fig. 11. E-plane radiation patterns generated by circular-sector patch oscillator of Fig. 7 $V_{\mathrm{ds}} = 2.3$ V.

Fig. 12. H-plane radiation patterns generated by circular-sector patch oscillator of Fig. 7 $V_{\mathrm{ds}} = 2.3$ V.
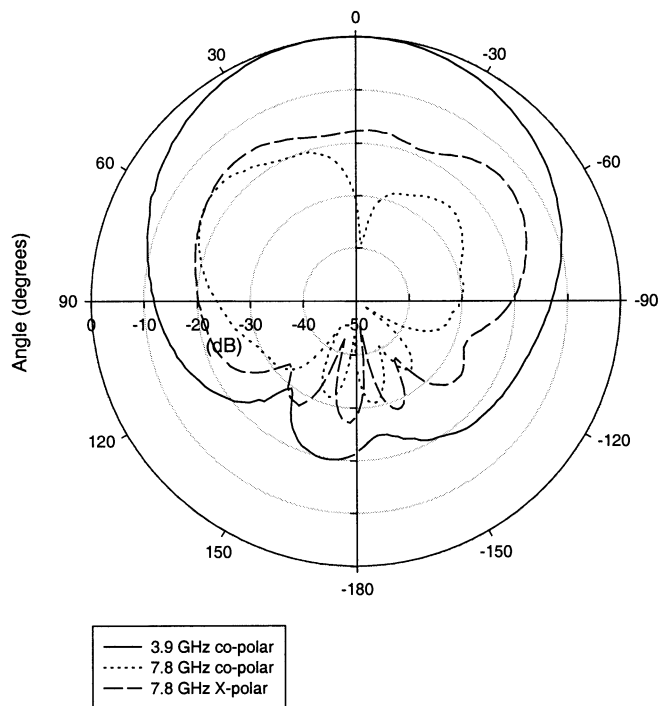

Fig. 13. E-plane radiation patterns generated by rectangular quarter-wave shorted rectangular patch oscillator of Fig. 8 $V_{\mathrm{ds}} = 2.2$ V.

this is most likely due to radiation from the oscillator circuitry. The harmonic levels are seen to be generally lower here. Figs. 11 and 12 show the radiation patterns for the circular-sector patch oscillator. Both E- and H-plane patterns are as one would expect for a circular-sector antenna [2]. There is no beam squint and a good front-to-back ratio. This may be due to the use of broad-band radial stubs instead of chip capacitors for gate biasing, as in the case of the rectangular patch. The harmonic radiation levels are much lower here, better than 18 dB at boresight
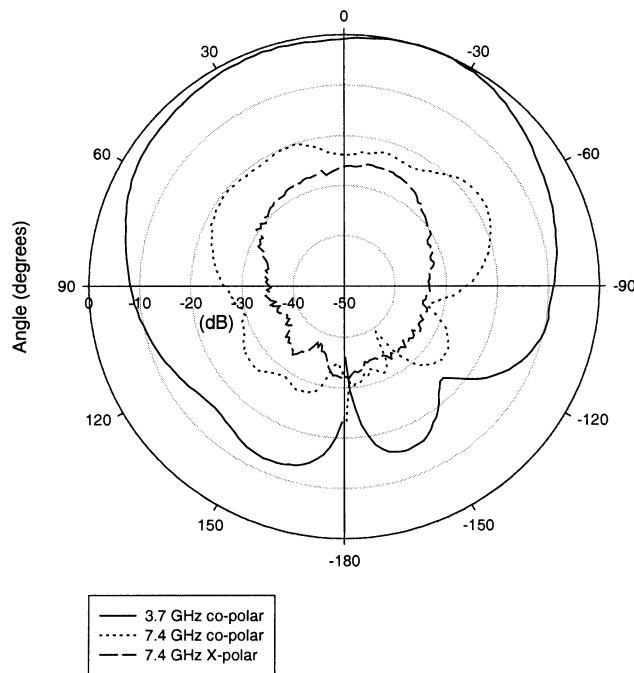
and better than 13 dB in the upper half-plane. Figs. 13 and 14 show the results for the quarter-wave shorted patch oscillator. Again, good fundamental radiation patterns are shown in both E- and H-planes. In this case, the harmonic suppression is further reduced to better than 21.4 dB on boresight and better than 17.1 dB in all of the upper half-plane. The performance of the three antennas is summarized in Table I.
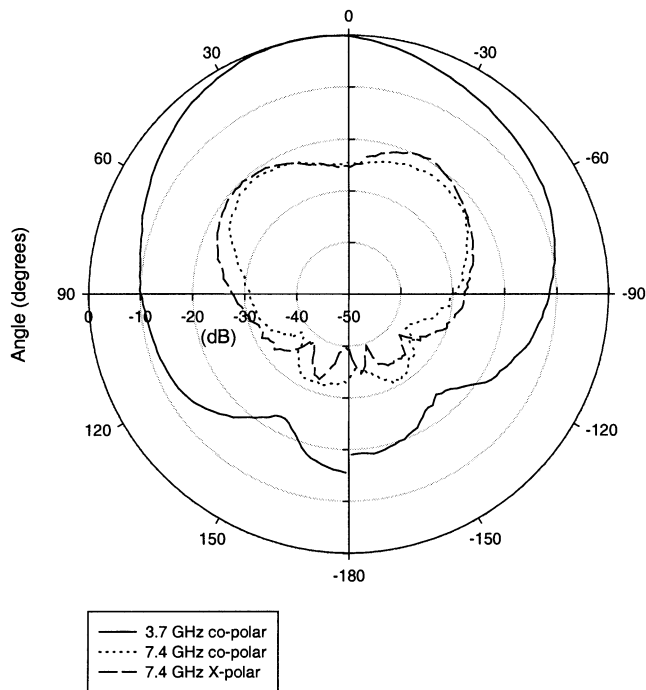
Fig. 14.　*H*-plane radiation patterns generated by rectangular quarter-wave shorted rectangular patch oscillator of Fig. 8 $V_{\rm ds} = 2.2$ V.

TABLE I
MEASURED MAXIMUM FIRST HARMONIC RADIATED POWER LEVELS
RELATIVE TO FUNDAMENTAL AT BORESIGHT FOR THREE
DIFFERENT TYPES OF PATCH OSCILLATOR

Patch Oscillator Type	Max. Harmonic Level Relative to Fundamental at Boresight (dB)							
	Boresight				Upper Half-Plane			
	E-Plane		H-Plane		E-Plane		H-Plane	
	Co	X	Co	X	Co	X	Co	X
Rectangular	-8.6	-10.7	-5.7	-10.7	-1.4	-10.0	-5.7	-5.7
Circular Sector	-30.0	-17.9	-30.0	-19.4	-15.7	-13.5	-29.4	-15.6
Quarter-Wave Shorted	-21.4	-24.3	-25.0	-25.0	-17.1	-23.5	-19.5	-20.7

In terms of input resistance, the rectangular patch will have the highest value; in the ideal case of a patch that is one wavelength long at the first harmonic frequency, the input resistance would be half of the radiation resistance and would be approximately 200 Ω for the patch shown in Fig. 6 [15]. In the case of the circular-sector patch, the input resistance is known to be very low at the first harmonic frequency [2], and the quarter-wave shorted patch will also be very low. Further work would be required to correlate the measured harmonic suppression with actual patch input resistances.

These results have shown that it is possible to reduce harmonic emissions from patch oscillators in the principle radiation planes by controlling the input resistance levels at the first harmonic frequencies. Full characterization of harmonic emission from patch antennas is a very demanding experimental task and will require full three-dimensional (3-D) radiation patterns.

VI. CONCLUSIONS

Harmonic radiation from patch oscillators has been investigated both theoretically and experimentally. Closed-form expressions for fundamental and first harmonic voltage amplitudes have been obtained for both single and dual LCR Van der Pol oscillators. They have been compared with a harmonic-balance analysis using MDS. In the single-resonator case, excellent agreement was found with MDS, but the levels of harmonic predicted were much lower than would be expected for patch oscillators. To improve the model, a second resonant circuit was introduced to model the first harmonic resonance of the patch. Here, reasonably good agreement was obtained with MDS and the harmonic levels were closer to those typically found in patch oscillators. The type of expressions obtained here can help to give the active antenna designer insights into the complex nature of these circuits without relying on time-consuming simulation on expensive commercial computer-aided design (CAD) packages. In particular, it has been shown that the first harmonic level will reduce with the input resistance of the antenna at that frequency.

The ideas proposed by the theoretical analysis have been experimentally investigated by constructing patch oscillators with antennas having different input resistances at the first harmonic frequency. The results presented show that best performance has been obtained with a quarter-wave shorted patch with radiative edge feeding, which will have very low first harmonic input resistance.

REFERENCES

[1] E. Elkhazmi, N. J. McEwan, and J. Moustafa, "Control of harmonic radiation from an active microstrip patch antenna," *J. Int. Nice Sur Les Antennas*, pp. 313–316, Nov. 1996.
[2] V. Radisic, Y. Qian, and T. Itoh, "Class F power amplifier integrated with circular sector microstrip antenna," in *IEEE MTT-S Int. Microwave Symp. Dig.*, Denver, CO, June 1997, pp. 687–690.
[3] A. Henderson, A. A. Abdulaziz, and J. R. James, "Microstrip planar array with interference suppression radome," *Electron. Lett.*, vol. 28, pp. 1465–1466, July 1992.
[4] K. C. Gupta and P. S. Hall, *Analysis and Design of Integrated Circuit Antenna Modules*, K. C. Gupta and P. S. Hall, Eds.　New York: Wiley, 1999.
[5] K. D. Stephan and W. A. Morgan, "Analysis of inter-injection-locked oscillators for integrated phased arrays," *IEEE Trans. Antennas Propagat.*, vol. AP-35, pp. 771–781, July 1987.
[6] R. Gillard, H. Legay, J. M. Floc'h, and J. Citerne, "A rigorous analysis of a receiving active microstrip antenna," *Electron. Lett.*, vol. 27, no. 25, pp. 2357–2359, Dec. 1991.
[7] M. Cryan, S. Helbing, F. Alimenti, P. Mezzanotte, L. Roselli, and R. Sorrentino, "Analysis and design of quasioptical multipliers using lumped element (LE) FDTD method," presented at the IEEE AP-S Symp., 1999.
[8] R. E. Mickens, *An Introduction to Non-Linear Oscillations*.　Cambridge, U.K.: Cambridge Univ. Press, 1985, pp. 32–55.
[9] B. Van der Pol, "The nonlinear theory of electric oscillations," *Proc. IRE*, vol. 22, no. 9, pp. 1051–1086, Sept. 1934.
[10] ——, "On oscillation hysteresis in a triode generator with two degrees of freedom," *Phil. Mag*, vol. 43, pp. 700–719, Sept. 1922.
[11] J. R. James, P. S. Hall, and C. Wood, *Microstrip Antenna Theory and Design*.　Stevenage, U.K.: Peregrinus, 1981.
[12] M. J. Cryan, P. S. Hall, K. S. H. Tsang, and J. Sha, "Integrated active antenna with full duplex operation," *IEEE Trans. Microwave Theory Tech*, vol. 45, pp. 1742–1748, Oct. 1997.
[13] T. Bercelli, *Nonlinear Active Microwave Circuits*.　Amsterdam, The Netherlands: Elsevier, 1987.
[14] G. D. Vendelin, A. M. Pavrio, and U. L. Rohde, *Microwave Circuit Design Using Linear and Nonlinear Techniques*.　New York: Wiley, 1990.
[15] D. Pozar, *PCAAD—Personal Computer Aided Antenna Design for Windows, Version 3.0*.　Leverett, MA: Antenna Design Assoc. Inc., 1996.

Martin J. Cryan (S'91–M'95–SM'01) received the B.Eng. degree in electronic engineering from The University of Leeds, Leeds, U.K., in 1986, and the Ph.D. degree from the University of Bath, Bath, U.K., in 1995.

He was a Microwave Design Engineer for five years following his undergraduate studies. From 1994 to 1997, he was a Researcher with the University of Birmingham, where he was involved with active integrated antennas. From 1997 to 1999, he was a European Community Training and Mobility Research (EC TMR) Research Fellow with the University of Perugia, Perugia, Italy, where he was involved with the design and simulation of quasi-optical multipliers using the lumped-element FDTD method. From 2000 to 2002, he was a Research Associate with the University of Bristol, Bristol, U.K., where he was involved with hybrid electromagnetic methods for electromagnetic compatibility (EMC) problems in optical transceivers and FDTD analysis of photonic crystals. He is currently a Lecturer with the Department of Electronic and Electrical Engineering, University of Bristol. His research interests include photonic crystals, active integrated antennas, FDTD analysis, and monolithic microwave integrated circuit (MMIC) design.

G. R. Buesnel, photograph and biography not available at time of publication.

Peter S. Hall (M'88–SM'93–F'01) received the Ph.D. degree in antenna measurements from Sheffield University, Sheffield, U.K., in 1973.

He then spent three years with Marconi Space and Defence Systems, Stanmore, U.K., where he was largely involved with a European Communications satellite project. He then joined The Royal Military College of Science as a Senior Research Scientist and progressed to Reader in electromagnetics. In 1994, he joined the University of Birmingham, Edgbaston, Birmingham, U.K., where he is currently a Professor of communications engineering and Head of the School and Head of the Communications Engineering Group, School of Electronic and Electrical Engineering. He has extensively performed research in the areas of microwave antennas and associated components and antenna measurements. He has authored or coauthored four books, over 130 learned papers, and holds various patents. From 1991 to 1995, he was an Honorary Editor of the *Proceedings of the Institution of Electrical Engineering, Part H*, and is currently an Editorial Board member of the *International Journal of RF and Microwave Computer Aided Engineering* and *Microwave and Optical Technology Letters*.

Dr. Hall is a Fellow of the Institution of Electrical Engineers (IEE), U.K. He is a past chairman of the IEE Antennas and Propagation Professional Group and of the organizing committee of the 1997 IEE International Conference on Antennas and Propagation. He has been associated with the organization of many international conferences and was a member of the Technical Committee of AP2000 in Switzerland and was an overseas corresponding member of ISAP2000 in Japan. He was the recipient of six IEE Premium Awards, including the 1990 IEE Rayleigh Book Award for the *Handbook of Microstrip Antennas*.